Available online at www.sciencedirect.com

Journal of Molecular Catalysis A: Chemical 246 (2006) 248–254

JOURNAL OF MOLECULAR CATALYSIS A: CHEMICAL

www.elsevier.com/locate/molcata

DRIFT study of internal donors in supported Ziegler–Natta catalysts

A.G. Potapov*, G.D. Bukatov, V.A. Zakharov

Boreskov Institute of Catalysis, Prospect Akademika Lavrentieva 5, Novosibirsk 630090, Russia

Received 11 October 2005; received in revised form 12 October 2005; accepted 10 November 2005
Available online 15 December 2005

Abstract

The state of internal donor (ID) in the supported titanium–magnesium ($TiCl_4$/ID/$MgCl_2$) catalysts for stereospecific propylene polymerization has been studied by diffuse reflectance infrared spectroscopy (DRIFT). The samples were prepared via interaction of highly dispersed $MgCl_2$ with different IDs (ethyl benzoate, EB; di-*n*-butyl phthalate, DBP) and $TiCl_4$. It was found that the DRIFT spectra of carbonyl groups of IDs adsorbed on $MgCl_2$ could be best described as a superposition of several overlapping vibration bands from a variety of surface complexes. Within this model the content of individual EB and DBP complexes on the $MgCl_2$ surface was calculated. In the case of EB, three main complexes were found on the $MgCl_2$ support in about equal proportions. In the case of DBP, only one of three complexes was preferentially formed. The surface content of both EB and DBP was found to decrease in presence of $TiCl_4$. At the same time $TiCl_4$ had influenced the distribution pattern of EB but not DBP complexes. The most likely scenario of competitive adsorption of $TiCl_4$ and IDs on the $MgCl_2$ support is discussed. A model describing surface distribution of $TiCl_4$ on $MgCl_2$ is proposed for $TiCl_4$/EB/$MgCl_2$ and $TiCl_4$/DBP/$MgCl_2$ catalysts.

Keywords: Ziegler–Natta polymerisation; Propylene; $MgCl_2$ support; DRIFT spectroscopy; Internal donor

1. Introduction

The internal donor (ID) is an important component in supported Ziegler–Natta catalysts for propylene polymerization responsible for stereospecificity of these catalysts [1–3]. It was demonstrated that the internal donor was strongly bound to the $MgCl_2$ support and did not interact with adsorbed $TiCl_4$ [4–7]. It is believed that the internal donor blocks particular sites on the $MgCl_2$ surface, which otherwise upon coordination with $TiCl_4$ would produce precursors of non-stereospecific active sites [4,8,9]. It was also suggested, that when adsorbed on the catalyst's surface the internal donor could convert aspecific active sites into specific ones [2,10–16]. Several theoretical studies have been performed to address the possible role of internal donors in Ziegler–Natta catalysts [17–19]. At the same time only limited experimental data on the distribution of the internal donor on the $MgCl_2$ support has been reported so far. One ^{13}C CP-MAS NMR study had found two esters (EB, ethyl benzoate and DIBP, di-iso-butyl phthalate) coordinated by non-equivalent surface sites on the $MgCl_2$ surface, with diester demonstrating somewhat different behaviour than monoester [6].

DRIFT spectroscopy is one of the most useful research tools in studying variety of surface species in solid catalysts. It can also be applied to probe the state of carbonyl groups in the molecules of internal donors, since the ν(C=O) adsorption band is very sensitive to coordination. Typical spectra of carbonyl groups of internal donors would have asymmetric shapes due to many different complexes co-existing on the surface [5,20–22]. In this work we have analyzed the ν(C=O) regions in the DRIFT spectra of samples prepared via interaction of highly dispersed $MgCl_2$ with EB (ethyl benzoate), DBP (di-*n*-butyl phthalate) and $TiCl_4$. Broad and asymmetric $\nu(c)$ bands were deconvoluted into several components from individual surface complexes involving internal donors. Using this approach it was possible to obtain quantitative information on the content of different complexes of EB and DBP. The likely mechanism of competitive adsorption of internal donors and $TiCl_4$ is discussed.

2. Experimental

2.1. Materials

Heptane, butylchloride, chlobenzene (PhCl), EB and DBP were used after dehydration over molecular sieves. All the preparation and manipulation with samples were performed under

---

* Corresponding author. Fax: +7 383 2 308056.
E-mail address: potapov@catalysis.nsk.su (A.G. Potapov).

1381-1169/$ – see front matter © 2005 Elsevier B.V. All rights reserved.
doi:10.1016/j.molcata.2005.11.016

argon atmosphere. Argon gas was additionally dried with molecular sieves and using a Drierite gas drying unit with anhydrous calcium sulfate.

2.2. *Support*

The highly dispersed $MgCl_2$ support was prepared via interaction of magnesium metal powder with C_4H_9Cl (molar ratio $C_4H_9Cl/Mg = 3$) in heptane at 98 °C with subsequent washing with heptane [23]. The resulting $MgCl_2$ support contained ca. 10 wt.% of organic residue and had a surface area of ca. 90 m^2/g.

2.3. *ID/$MgCl_2$ samples*

The $MgCl_2 \cdot 0.35EB$, $MgCl_2 \cdot 0.1EB$, $MgCl_2 \cdot 0.35DBP$ and $MgCl_2 \cdot 0.1DBP$ samples were prepared by interaction of a suspension of $MgCl_2$ in heptane (2.5 ml/g of $MgCl_2$) with corresponding ester (loading ester/$MgCl_2$ molar ratio of 0.35:1 for the $MgCl_2 \cdot 0.35ID$ samples and 0.1:1 for the $MgCl_2 \cdot 0.1ID$ samples) at 103 °C for 5 h. The samples were washed twice with heptane.

The EB/$MgCl_2$ (−50 °C) and DBP/$MgCl_2$ (−50 °C) samples were prepared by dosing ester (EB/Mg ratio of 0.0057 and DBP/Mg ratio of 0.00085 and 0.0017) to a suspension of $MgCl_2$ in heptane (25 ml/g of $MgCl_2$) at −50 °C for 0.5 h. After dosing, the temperature was increased to 20 °C and the reaction mixture was kept at this temperature for 1 h.

The EB/$MgCl_2$ (20 °C) and DBP/$MgCl_2$ (20 °C) samples were prepared by dosing ester (EB/Mg ratio of 0.014 and 0.028 and DBP/Mg ratio of 0.014) to a suspension of $MgCl_2$ in heptane (25 ml/g of $MgCl_2$) at 20 °C for 0.5 h and kept at this temperature for 1 h. The samples were washed once with heptane.

The EB/$MgCl_2$ (105 °C) sample was prepared by adding EB to a suspension of $MgCl_2$ (EB/$MgCl_2$ = 0.1) in PhCl (25 ml/g of $MgCl_2$) at 105 °C and keeping the reaction mixture at this temperature for 1 h. The resulted sample was washed once with PhCl at 105 °C and twice with heptane.

The DBP/$MgCl_2$ (115 °C) sample was prepared by adding DBP to a suspension of $MgCl_2$ (DBP/$MgCl_2$ = 0.07) in PhCl (25 ml/g of $MgCl_2$) at 115 °C and keeping the reaction mixture at this temperature for 1 h. The resulted sample was washed once with PhCl at 115 °C and twice with heptane.

2.4. *Catalysts*

Titanium–magnesium catalyst (**I**) with a composition of $TiCl_4$/EB/$MgCl_2$ (0.77 wt.% of Ti, 1.5 wt.% of EB) was prepared via treatment of $MgCl_2$ with a mixture of $TiCl_4$/PhCl (1:1 vol., Ti/Mg = 10) in presence of EB (EB/$MgCl_2$ = 0.1) at 105 °C for 1 h and followed by two treatments with the same $TiCl_4$/PhCl mixture at 105 °C for 0.5 h. The catalyst was washed once with PhCl and three times with heptane.

Titanium–magnesium catalyst (**II**) with a composition of $TiCl_4$/DBP/$MgCl_2$ (0.82 wt.% of Ti, 2.8 wt.% of DBP) was prepared via treatment of $MgCl_2$ with a mixture of $TiCl_4$/PhCl (1:1 vol., Ti/Mg = 10) in presence of DBP (DBP/$MgCl_2$ = 0.07) at 115 °C for 1 h and followed by two treatments with the same $TiCl_4$/PhCl mixture at 115 °C for 1 and 0.5 h. The catalyst was washed once with PhCl and three times with heptane.

2.5. *Chemical analysis*

Titanium content in the samples was determined with inductively coupled plasma-atomic emission spectrometry (ICP-AES). To determine DBP content the samples were suspended in heptane and decomposed by 10% H_2SO_4. The organic phase was separated, washed twice with distilled water, dried and weighted. The EB content was determined by GC analysis of the organic phase after hydrolysis of the samples in heptane with 10% H_2SO_4.

2.6. *DRIFT measurements*

Prior to DRIFT measurements all samples were dried in vacuum at room temperature. The DRIFT spectra were recorded on a Bruker Vector 22 FT-IR spectrometer equipped with a dry nitrogen chamber and sealed cells with CaF_2 windows. All spectra were recorded with a nominal resolution of 4 cm^{-1}.

3. Results and discussion

3.1. *Interaction of EB with $MgCl_2$*

On the surface of highly dispersed polycrystalline $MgCl_2$ there are three types of low-coordinated Mg ions, i.e. $\mathbf{Q^5}$ sites, five-coordinated Mg ions at the (1 0 0) face; $\mathbf{Q^4}$, four-coordinated Mg ions at the (1 1 0) face, and $\mathbf{Q^3}$, three-coordinated Mg ions at the edges and corners of $MgCl_2$ crystals [8,10]. These low-coordinated Mg ions demonstrate pronounced Lewis acidic properties and are capable of strong coordination of ester molecules, including EB and DBP internal donors studied in this work. Since there are several different Mg sites on the $MgCl_2$ surface, it is typical to observe several types of carbonyl groups in the corresponding IR spectra of adsorbed IDs [24]. The individual c absorption bands would often overlap and produce a broad asymmetric feature covering the whole range of vibrations of carbonyl groups. As an example, the DRIFT spectra of the $MgCl_2 \cdot 0.35EB$ and $MgCl_2 \cdot 0.1EB$ samples (see Section 2) are shown in Fig. 1. In this spectrum the absorption bands of carbonyl groups $\nu(c)$ can be seen in the range of 1600–1750 cm^{-1} with at least four distinct maxima at ca. 1649, 1675, 1697 and 1724 cm^{-1}. The band at 1724 cm^{-1} is close to the $\nu(c)$ carbonyl stretching vibrations in neat EB ester (ca. 1720 cm^{-1}) and can be attributed to carbonyl groups in loosely coordinated EB or EB in $MgCl_2 \cdot 1EB$ and $MgCl_2 \cdot 2EB$ complexes [22]. On the other hand it is known, that upon coordination of ester molecules to metal ions via carbonyl oxygen, the corresponding $\nu(c)$ frequencies would decrease relative to free ester [5]. Thus, we suggest that three remaining c bands in the DRIFT spectrum of this sample are most likely from three distinct types of EB species bound strongly to $\mathbf{Q^3}$–$\mathbf{Q^5}$ Mg ions of $MgCl_2$. The ratio between individual complexes can be determined via computer-assisted deconvolution of the DRIFT spectra into separate bands. In this work such deconvo-

Table 1
The EB-containing samples synthesized and studied in this work

Sample	EB loading[a] (μmol/g)	EB content[b]		Ti content[b] (μmol/g)	Relative amount (% of total) of carbonyl groups at (cm^{-1})[c]				
		wt.%	μmol/g		1645	1675	1695	1717–1724	1737
(1) $MgCl_2$·0.35EB	3670	35.5	3670	–	23	29	14	34	–
(2) $MgCl_2$·0.1EB	1050	13.6	1050	–	37	18	26	19	–
(3) EB/$MgCl_2$ (−50 °C)	60	0.9	60	–	27	46	27	0	–
(4) EB/$MgCl_2$ (20 °C)	150	2.2	150	–	32	27	36	5	–
(5) EB/$MgCl_2$ (20 °C)	300	3.9	260	–	22	46	25	7	–
(6) EB/$MgCl_2$ (105 °C)	950	3.6	240	–	19	46	22	6	7
(7) Catalyst (**I**)	950	1.5	100	160	24	71	3	–	2

[a] In the reaction mixture.

[b] Determined by chemical analysis.

[c] Determined via deconvolution of DRIFT spectra (see text).

lution (Table 1) has been performed based on a Gaussian shape of the adsorption bands and on an assumption that each carbonyl band in the spectrum had the same extinction coefficient. It was found, the bands positions used for deconvolution do not depend on the composition of samples 1 and 2 in spite of significant differences in EB content and can be obviously used as start position for deconvolution of spectra of other samples studied in this work.

We have also prepared a series of four EB/$MgCl_2$ samples with progressively increased EB contents ranging from 1 to ca. 4 wt.% (samples 3–6, Table 1). The preparation procedure has been chosen to increase EB/Mg ratio and temperature at adsorption of EB on $MgCl_2$. In the samples 3 and 4 the quantity of adsorbed EB was equal to the quantity of EB used for adsorption. It is important that in samples 5 and 6 the amount of adsorbed EB was very close, or about 250 μmol/g, as determined by the chemical analysis, despite almost three-fold difference in the EB loading in the reaction mixture and considerably higher reaction temperature for the latter (see Section 2, Table 1). We believe, that the loading of ca. 250 μmol/g was the saturation level for EB adsorbed on used $MgCl_2$ under our experimental conditions, above which no further EB adsorbtion was possible. This value is slightly higher than the content of Lewis acidic sites estimated via low temperature adsorption of CO on a similar $MgCl_2$ sample (180 μmol/g) [25]. The difference is likely due to incomplete coverage of centers with low acidity with CO. Note, much higher the EB content in samples 1 and 2 is due to other conditions of their preparation (higher (one order) concentration of reagents, other solvent) resulting in more profound interaction of EB and $MgCl_2$ with a partial disintegration of $MgCl_2$ structure.

The DRIFT spectra for the samples 3–6 are compared in Fig. 2. Similarly to the above-discussed DRIFT spectra of the $MgCl_2{\cdot}n$EB samples (Fig. 1), the *c* adsorption band in these samples is very broad and asymmetric indicating presence of several types of surface complexes in slightly different relative proportions. Based on the deconvolution model proposed for the $MgCl_2{\cdot}n$EB samples, these DRIFT spectra can also be presented as a superposition of three major components at ca. 1645, 1675 and 1695 cm^{-1} (Figs. 2 and 3) (note absence of loosely coordinated EB in these samples). For the samples 4–6 an additional adsorption band of low intensity at ca. 1717 cm^{-1} can be seen, and in the sample 6 prepared at high temperature a small shoulder at ca. 1737 cm^{-1} was also found. Results of

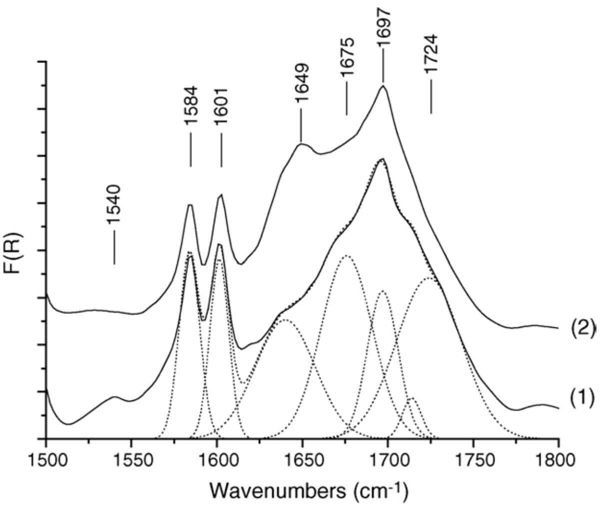

Fig. 1. DRIFT spectra of $MgCl_2$·0.35EB (1) and $MgCl_2$·0.1EB (2) samples. An example of the spectrum deconvolution is shown for the $MgCl_2$·0.35EB sample.

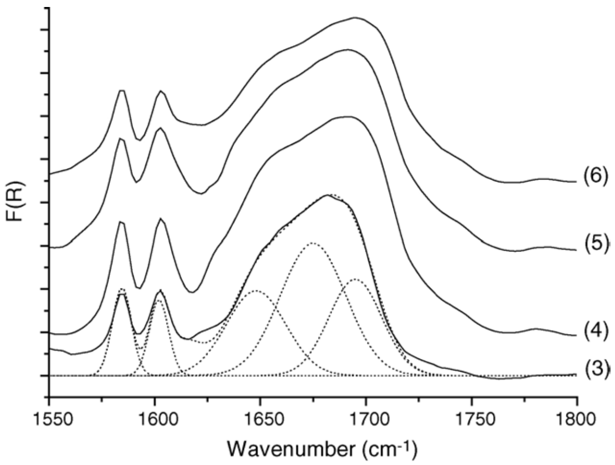

Fig. 2. DRIFT spectra of the samples containing EB. The spectra are labeled according to Table 1. The first spectrum is shown with its deconvolution into individual components.

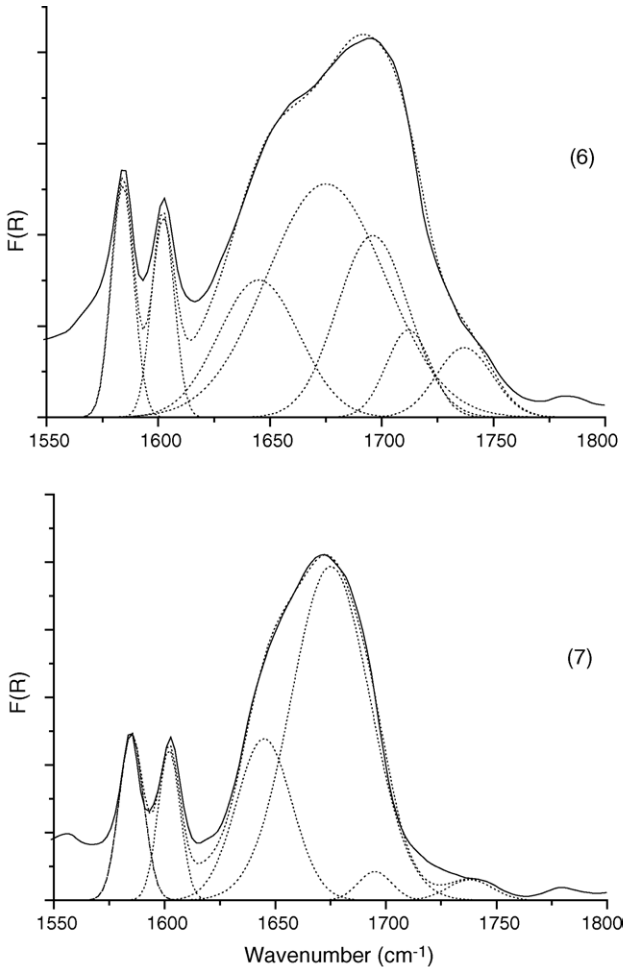

Fig. 3. DRIFT spectra of the EB/$MgCl_2$ sample (6) and catalyst (**I**) (7) (samples 6 and 7 in Table 1) demonstrating effect of $TiCl_4$ on the distribution of EB over $MgCl_2$ surface.

the computer-assisted deconvolution of these DRIFT spectra are summarized in Table 1.

As has been mentioned above, three major types of EB species detected in the DRIFT spectra of EB/$MgCl_2$ samples most likely correspond to three types of surface-exposed Mg ions in different chlorine coordination, $\mathbf{Q^5}$, $\mathbf{Q^4}$ and $\mathbf{Q^3}$. It is understood, that the Lewis acidity of these ions would increase as $\mathbf{Q^5} < \mathbf{Q^4} < \mathbf{Q^3}$ while the $\nu(c)$ frequency for surface EB·$\mathbf{Q^n}$ complexes is likely to decrease in the same direction. Thus, individual c bands detected in the DRIFT spectra can be tentatively attributed to particular surface EB complexes: EB·$\mathbf{Q^5}$ at 1695 cm^{-1}, EB·$\mathbf{Q^4}$ at 1675 cm^{-1} and EB·$\mathbf{Q^3}$ at 1645 cm^{-1}.

Relative amounts of EB·$\mathbf{Q^n}$ complexes in the studied EB/$MgCl_2$ samples as determined via deconvolution of the DRIFT spectra (Fig. 2) are summarized in Table 1. The sample 3 prepared at −50 °C shows that at low temperatures EB would form predominately EB·$\mathbf{Q^4}$ complexes with $\nu(c)$ at 1675 cm^{-1}. In the sample 4 all three surface complexes were populated in about equal proportions. In the samples 5 and 6, where the saturation EB loading was achieved (see above), the DRIFT spectra as well as their deconvolutions were remarkably close, indicating that similar complexes and in similar ratios were formed regardless of preparation conditions.

3.2. Interaction of EB with $MgCl_2$ in presence of $TiCl_4$

It is clear, that in real titanium–magnesium catalysts of propylene polymerization the active component, $TiCl_4$, will affect the distribution of EB over $MgCl_2$ surface. To investigate these effects, a catalyst sample with a composition of $TiCl_4$/EB/$MgCl_2$ was prepared under the same conditions (as to temperature, EB/Mg ratio, duration and solvents) as have been used to synthesize the EB/$MgCl_2$ sample 6 (see Section 2). The chemical analysis data indicate, that when the treatment of $MgCl_2$ with EB was performed in presence of $TiCl_4$, the amount of adsorbed EB was considerably lower (Table 1). At the same time the total number of surface species (EB and $TiCl_4$) found in the catalyst was very close to the EB content in the EB/$MgCl_2$ sample, 260 and 240 μmol/g, respectively. This observation suggests, that the lower EB content in the catalyst (**I**) is most likely a result of competition of $TiCl_4$ and EB for the same surface adsorption sites.

DRIFT spectra of two samples are compared in Fig. 3. The spectra are notably different due to different distribution patterns of EB complexes in two systems (Table 1). In the catalyst (**I**) EB exists mainly as EB·$\mathbf{Q^4}$ complexes (71%) and only 24% as EB·$\mathbf{Q^3}$ complexes, while the number of EB·$\mathbf{Q^5}$ complexes in this catalyst was very low (not exceeding 3%). Two sets of data, DRIFT and the chemical analysis, have allowed us to identify most plausible localization of $TiCl_4$ and EB species on different crystallographic faces of $MgCl_2$ crystals (Table 2).

Perhaps the most important observation was that the complexes of EB with $\mathbf{Q^5}$ ions were almost totally eliminated in presence of $TiCl_4$. There was also moderate (by ca. 40%) removal of EB·$\mathbf{Q^4}$ and EB·$\mathbf{Q^3}$ complexes. Thus, it becomes clear that $TiCl_4$ may indeed substitute or prevent interaction of EB with all three types of Mg ions. $TiCl_4$ predominately substitutes complexes of EB with $\mathbf{Q^5}$ ions, while the most preferable interaction of EB in presence of $TiCl_4$ is with $\mathbf{Q^4}$ ions. In this sample $TiCl_4$ species occupy almost all available $\mathbf{Q^5}$ adsorption sites at the (1 0 0) face of $MgCl_2$, when at the (1 1 0) face such species are likely to have EB species in their nearest surrounding (EB/Ti ratio for this face is 1.76). About 15% of $TiCl_4$ molecules is coordinated by $\mathbf{Q^3}$ Mg ions and would also contain EB in their nearest surrounding (EB/Ti ratio is 1.17).

Table 2
The distribution of EB and $TiCl_4$ complexes on $MgCl_2$ for samples 6 and 7 in Table 1

Sample	*X* distribution (μmol/g)				
	X	Total	*X* on $\mathbf{Q^3}$	*X* on $\mathbf{Q^4}$	*X* on $\mathbf{Q^5}$
EB/$MgCl_2$ (105 °C)	EB	240	45	111	53
EB/$TiCl_4$/$MgCl_2$ (catalyst (**I**))	EB	100	24	71	3
	$TiCl_4$	140	21[a]	40[a]	50[a]
	EB/$TiCl_4$	0.71	1.2	1.76	0.05

[a] Calculated as ΔEB = EB (in EB/$MgCl_2$) − EB (in catalyst (**I**)).

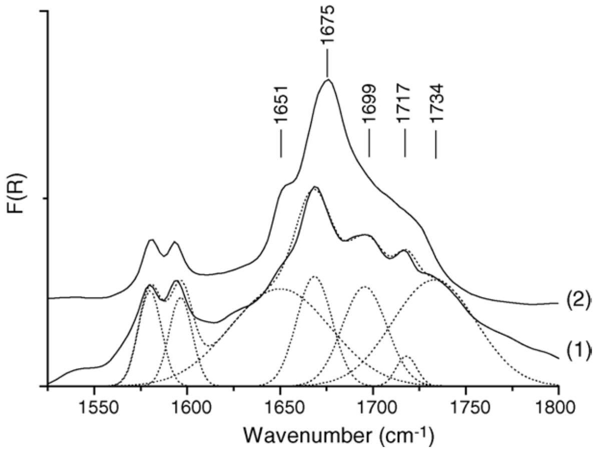

Fig. 4. DRIFT spectra of $MgCl_2 \cdot 0.35DBP$ (1) and $MgCl_2 \cdot 0.1DBP$ (2) samples. An example of the spectrum deconvolution is shown for the $MgCl_2 \cdot 0.35DBP$ sample.

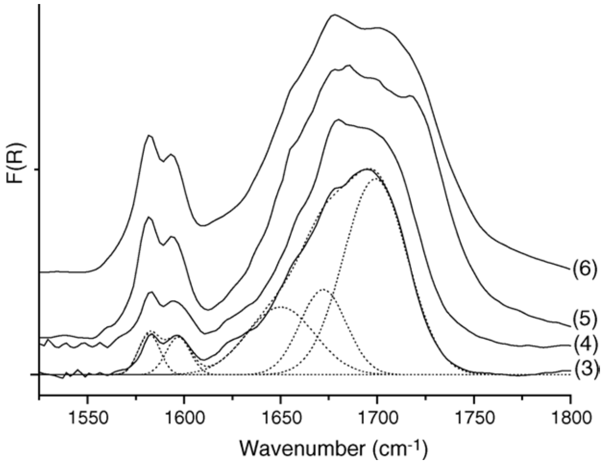

Fig. 5. DRIFT spectra of the samples containing DBP. The spectra are labeled according to Table 3. The first spectrum is shown with its deconvolution into individual components.

3.3. Interaction of DBP with $MgCl_2$

The DRIFT spectra of $MgCl_2 \cdot 0.35DBP$ and $MgCl_2 \cdot 0.1DBP$ samples prepared in excess of DBP were very complicated with several pronounced maxima (Fig. 4). These spectra can be best represented as a superposition of at least five separate bands at ca. 1650, 1672, 1699, 1722 and 1734 cm^{-1} (Fig. 4(1)). The bands at 1650, 1672 and 1699 cm^{-1} are most likely from complexes of DBP with surface acidic sites of $MgCl_2$, since formation of such complexes would decrease the $\nu(c)$ vibration frequency comparing with neat ester (ca. 1728 cm^{-1} in liquid DBP and 1760 cm^{-1} in the gas phase). The bands at 1722 and 1734 cm^{-1} may indicate presence of free or weakly bound carbonyl groups of ester molecules. The ratio between different carbonyl species depends on the composition of $MgCl_2 \cdot n$DBP samples. Note here, similarly to EB containing samples the bands positions do not depend on the composition of samples. In the sample with lower ester content ($MgCl_2 \cdot 0.1DBP$) the share of complexes in the low frequency range (1650–1700 cm^{-1}) was higher (Fig. 4). This observation supports earlier suggestion, that the c absorption bands at lower frequency correspond to stronger complexes of esters with Mg ions. Indeed, such sites are first to be occupied at lower ester loadings.

In DBP/$MgCl_2$ samples prepared via controlled addition of ester to $MgCl_2$ (Table 3, samples 3–6) only surface DPB complexes were expected to form. The shape of DRIFT spectra for these samples depends on the DBP loading and synthesis conditions (Fig. 5) similarly to the EB/$MgCl_2$ system. Using the same approach these DRIFT spectra were deconvoluted using band positions found for $MgCl_2 \cdot 0.35DBP$ and $MgCl_2 \cdot 0.1DBP$ samples. The deconvolution data are summarized in Table 3. It is interesting, that in all studied DBP/$MgCl_2$ samples only a single predominant complex of DBP at $\nu(c) = 1699$ cm^{-1} was apparently formed with 53–76% of the total intensity. The share of two other complexes with $\nu(c)$ at 1672 and 1650 cm^{-1} had varied from 9 to 25%.

Unlike the case of EB, for DBP it was difficult to attribute observed $\nu(c)$ bands to particular DBP complexes with Mg ions: DBP molecules have two carbonyl groups and may interact either with single Mg ion producing chelated complex or with two Mg ions producing bridged complex. Thus, the correlation between the number of chlorine vacancies at Mg ions and the $\nu(c)$

Table 3
The DBP-containing samples synthesized and studied in this work

Sample	DBP loading[a] (μmol/g)	DBP content[b]		Ti content[b] (μmol/g)	Relative amount (% of total) of carbonyl groups at (cm^{-1})[c]				
		wt.%	μmol/g		1650	1672	1699	1722–1734[d]	1752[e]
(1) $MgCl_2 \cdot 0.35DBP$	3670	50.5	3670	–	36	14	16	34	–
(2) $MgCl_2 \cdot 0.1DBP$	1050	22.6	1050	–	14	39	37	10	–
(3) DBP/$MgCl_2$ (−50 °C)	9	0.25	9	–	22	18	60	–	–
(4) DBP/$MgCl_2$ (−50 °C)	18	0.5	18	–	18	15	67	–	–
(5) DBP/$MgCl_2$ (20 °C)	150	4.2	150	–	11	9	76	4	–
(6) DBP/$MgCl_2$ (115 °C)	660	7.0	250	–	25	10	53	12	–
(7) Catalyst (**II**)	660	2.8	110[f]	170	19	10	45	–	26

[a] In the reaction mixture.
[b] Determined by chemical analysis.
[c] Determined via deconvolution of DRIFT spectra (see text).
[d] Free or weakly bound carbonyl groups of DBP.
[e] Phthaloyl chlorides.
[f] As the sum of −COO and COCl groups.

frequencies may be somewhat different from what was found for EB. Recent quantum chemical calculations has also suggested presence of both chelated and bridged complexes of phthalate on (1 1 0) face of $MgCl_2$ surface [19]. The absolute energy of bridged phthalate complexes was lower at the (1 1 0) than at (1 0 0) face, while formation of chelated complexes at the (1 1 0) face was found less preferable then formation of bridged complexes at the (1 0 0) face. These most recent quantum chemical calculation data correlate well with earlier studies [17].

Based on these results, we may suggest two possible interpretations of DRIFT spectra recorded in the $DBP/MgCl_2$ system. (i) The attribution similar to the $EB/MgCl_2$ system, i.e. the complexes with $\nu(c)$ frequencies of 1699 and 1672 cm^{-1} are the complexes of DBP with $\mathbf{Q^5}$ and $\mathbf{Q^4}$ ions, respectively. The complexes with $\mathbf{Q^5}$ ions are most likely of bridged type, while complexes with $\mathbf{Q^4}$ ions can be either chelated (two carbonyl groups per Mg ion) or bridged (two carbonyl groups per two Mg ions). Note, in this case similar frequencies of DBP and EB carbonyl groups with Mg ioms are observed (for instance, 1699 and 1695 cm^{-1} with $\mathbf{Q^5}$ Mg ions, respectively). (ii) The second possibility would be to assign the band at 1699 cm^{-1} to chelated DBP complexes with $\mathbf{Q^4}$ Mg ions while the band at 1672 cm^{-1} to bridged DBP complexes with $\mathbf{Q^5}$ ions. This possibility corresponds to literature data on the preferable coordination of an internal donor on the (1 1 0) face of $MgCl_2$ ($\mathbf{Q^4}$ ions) [8,26,27].

Thus, presented DRIFT data does not allow us to make conclusive attributions of the observed $\nu(c)$ bands to any particular type of surface DBP. At this moment we are performing quantum chemical simulations of the IR spectra for EB and DBP complexes with different types of Mg ions. We believe these results would help in selecting most plausible configurations of surface complexes of internal donors.

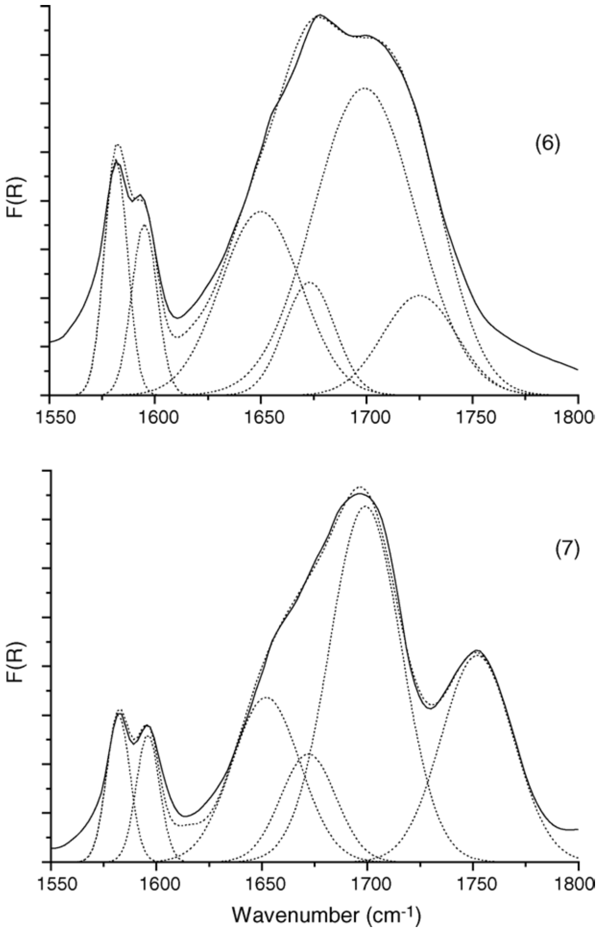

Fig. 6. DRIFT spectra of the $DBP/MgCl_2$ sample (6) and catalyst (**II**) (7) (samples 6 and 7 in Table 3) demonstrating effect of $TiCl_4$ on the distribution of DBP over $MgCl_2$ surface.

3.4. *Interaction of DBP with $MgCl_2$ in presence of $TiCl_4$*

The $TiCl_4/DBP/MgCl_2$ catalyst (sample 7) was prepared under the same conditions as the $DBP/MgCl_2$ sample 6. The DRIFT spectra of these two samples are compared in Fig. 6. According to the chemical analysis (Table 3), presence of $TiCl_4$ resulted in a drastic decrease of the total DBP content in the catalyst sample, with both $TiCl_4$ and DBP competing for the same $MgCl_2$ sites, similarly to the catalyst (**I**) containing EB. The total content of the surface species (DBP and $TiCl_4$) was similar in the catalyst (**II**) and in the $DBP/MgCl_2$ sample 6, 280 and 250 µmol/g, respectively. In the catalyst (**II**) significant part of DBP was converted into phthaloyl chlorides as supported by the presence of the characteristic DRIFT band at ca. 1752 cm^{-1} from COCl groups (Fig. 6) [21]. The latter feature was the main difference between the $DBP/MgCl_2$ sample 6 and the catalyst (**II**), while the distribution patterns of carbonyl groups among different sites were similar for two samples (Table 3). The complexes of DBP characterized by $\nu(c)$ of 1699 cm^{-1} had dominated in both cases.

Table 4
The distribution of DBP and $TiCl_4$ complexes on $MgCl_2$ for samples 6 and 7 in Table 3

Sample	*X* distribution (µmol/g)				
	X	Total	At the place of DBP complexes with $\nu(c)$ of cm^{-1}		
			1650	1672	1699
$DBP/MgCl_2$ (115 °C)	DBP	250	63	25	133
$DBP/TiCl_4/MgCl_2$ (catalyst (**II**))	DBP	110[a]	21	11	50
	$TiCl_4$	140	42[b]	14[b]	83[b]
	$DBP/TiCl_4$	0.79	0.50	0.78	0.60

[a] Including phthaloyl chlorides.
[b] Calculated as ΔDBP = DBP (in $DBP/MgCl_2$) - DBP (in catalyst (**II**)).

It was possible to quantify distribution of DBP complexes on $MgCl_2$ in presence and absence of $TiCl_4$ (Table 4). Different types of DBP complexes were replaced with $TiCl_4$ in close proportions contrary to the catalyst (**I**) containing EB, where favorable removal of only one type of complexes was observed (Table 2). In the total the $TiCl_4$ complexes are distributed on different Mg ions in the proportion 3:1:6 (Table 4) at the places of DBP complexes possessing with $\nu(c)$ of 1650, 1672 and 1699 cm^{-1}, correspondingly. $TiCl_4$ complexes adsorbed on different Mg ions could contain DBP in their nearest surrounding (the DBP/Ti ratio at all ions is 0.5–0.78).

4. Conclusion

It has been established that the internal donors (EB and DBP) could form different surface complexes on the $MgCl_2$ support, in particular, with three-, four- or five-coordinated Mg ions ($\mathbf{Q^3}$, $\mathbf{Q^4}$ or $\mathbf{Q^5}$). In the case of EB these complexes were formed in close proportions. In the case of DBP formation of only one type of complexes was most preferable. In presence of $TiCl_4$ the surface complexes of EB were formed mostly with Mg($\mathbf{Q^4}$) ions. At the same time $TiCl_4$ had not affected the distribution pattern of DBP complexes on the $MgCl_2$ support. In both cases presence of $TiCl_4$ resulted in considerable decrease in the total content of internal donor. Apparent competition of the internal donor and $TiCl_4$ for the same surface adsorption sites has allowed us to probe the distribution of $TiCl_4$ on different Mg ions. This information readily accessible via DRIFT spectroscopy may be useful in understanding different catalytic behavior of catalysts prepared with EB and DBP internal donors, and further in developing more effective $TiCl_4$/ID/$MgCl_2$ catalytic systems.

Acknowledgement

We are grateful to Dr. Victor Terskikh (University of Ottawa, Canada) for valuable comments.

References

[1] E. Albizzati, U. Giannini, G. Collina, L. Noristi, L. Resconi, in: E.P. Moore Jr. (Ed.), Polypropylene Handbook. Polymerization, Characterization, Properties, Applications, Hanser Publishers, Munich-Vienna-New York, 1996 (Chapter 2).

[2] J.C. Chadwick, Macromol. Symp. 173 (2001) 21.

[3] G. Cecchin, G. Morini, A. Pelliconi, Macromol. Symp. 173 (2001) 195.

[4] S.A. Sergeev, G.D. Bukatov, V.A. Zakharov, E.M. Moroz, Makromol. Chem. 184 (1983) 2421.

[5] M. Terano, T. Kataoka, T. Keii, in: T. Keii, K. Soga (Eds.), Catalytic Polymerization of Olefins, Kodansha-Elsevier, Amsterdam, 1986, p. 407.

[6] P. Sormunen, T. Hjertberg, E. Iiskola, Makromol. Chem. 191 (1990) 2663.

[7] M. Terano, M. Saito, T. Kataoka, Makromol. Chem. Rapid Commun. 13 (1992) 103.

[8] V. Busico, P. Corradini, L. DeMartino, A. Proto, V. Savino, E. Albizzati, Makromol. Chem. 186 (1985) 1279.

[9] M.C. Sacchi, I. Tritto, C. Shan, R. Mendichi, L. Noristi, Macromolecules 24 (1990) 6823.

[10] V. Busico, P. Corradini, A. Ferraro, A. Proto, Makromol. Chem. 187 (1986) 1125.

[11] K. Soga, T. Shiono, Y. Doi, Makromol. Chem. 189 (1988) 1531.

[12] M.C. Sacchi, F. Forlini, I. Tritto, R. Mendichi, G. Zannoni, Macromolecules 25 (1992) 5914.

[13] G.D. Bukatov, V.A. Zakharov, Macromol. Chem. Phys. 202 (2001) 2003.

[14] J.C. Chadwick, G. Morini, G. Balbontin, I. Camurati, J.J.R. Heere, I. Mingozzi, F. Testoni, Macromol. Chem. Phys. 202 (2001) 1995.

[15] V. Busico, R. Cipullo, G. Monaco, G. Talarico, M. Vacatello, J.C. Chadwick, A.L. Segre, O. Sudmeijer, Macromolecules 32 (1999) 4173.

[16] B. Liu, T. Nitta, H. Nakatani, M. Terano, Macromol. Chem. Phys. 204 (2003) 395.

[17] L. Barino, R. Scordamaglia, Macromol. Symp. 89 (1995) 101.

[18] E. Puhakka, T.T. Pakkanen, T.A. Pakkanen, J. Mol. Catal. A Chem. 123 (1997) 171.

[19] A. Correa, G. Talarico, G. Morini, L. Cavallo, in: M. Terano (Ed.), Current Achievements on Heterogeneous Olefin Polymerization Catalysts, Sankeisha Co. Ltd., Nagoya, 2004, p. 44.

[20] A. Guyot, R. Spitz, L. Duranel, J.L. Lacombe, in: T. Keii, K. Soga (Eds.), Catalytic Polymerization of Olefins, Kodansha-Elsevier, Amsterdam, 1986, p. 147.

[21] G.G. Arzoumanidis, N.M. Karayannis, Appl. Catal. 76 (1991) 221.

[22] M. Ystenes, Ø Bache, O.M. Bade, R. Blom, J.L. Eilertsen, Ø. Nirisen, M. Ott, K. Svendsen, E. Rytter, in: M. Terano, T. Shiono (Eds.), Future Technology for Polyolefin and Olefin Polymerization Catalysis, Technology and Education Publishers, Tokyo, 2002, p. 184.

[23] USSR Patent 726702 (1978), V.A.Zakharov, S.I.Makhtarulin (invs.), Chem. Abstr. 95, 1981. 220579x.

[24] E. Albizzati, M. Galimberti, U. Giannini, G. Morini, Makromol. Chem. Makromol. Symp. 48–49 (1991) 223.

[25] V.A. Zakharov, E.A. Paukshtis, T.B. Mikenas, A.M. Volodin, E.N. Vitus, A.G. Potapov, Macromol. Symp. 89 (1995) 55.

[26] M.C. Sacchi, F. Forlini, I. Tritto, P. Locatelli, G. Morini, L. Noristi, E. Albizzati, Macromolecules 29 (1996) 3341.

[27] J.C. Chadwick, G. Morini, G. Balbontin, I. Mingozzi, E. Albizzati, O. Sudmeijer, Macromol. Chem. Phys. 198 (1997) 1181.